Romanian Reports in Physics **69**, 408 (2017)

NONSTATIONARY EXPONENTIAL DISTRIBUTIONS OF THE STATISTICAL BREAKDOWN TIME DELAY IN ARGON DC GLOW DISCHARGE AT LOW PRESSURE

S.N. STAMENKOVIĆ*, V. LJ. MARKOVIĆ, A.P. JOVANOVIĆ, M.N. STANKOV

University of Niš, Faculty of Sciences and Mathematics, Department of Physics, 18000 Niš, Višegradska 33, P.O. Box 224, Serbia, *E-mail: ssuzana@pmf.ni.ac.rs

Received April 25, 2016

Abstract. The experimental distributions of statistical breakdown time delay t_s in argon DC glow discharge, with unconditioned electrodes, at low pre-ionization levels are presented. Because of low level of residual particles exponential distributions are expected. However, the data deviate from expected distributions and for their description the nonstationary exponential distribution with time dependent distribution parameter YP that reflects unstable experimental conditions, is necessary (Y is electron yield, P the breakdown probability). For data analysis, Laue diagrams, cumulative, as well as density distributions are used. The obtained data are also fitted by the stationary exponential and Weibull distributions for the sake of comparison.

Key words: nonstationary exponential distribution, time dependent distribution parameter, electrical breakdown, statistical time delay.

1. INTRODUCTION

The electrical processes and phenomena in gases have been intensively studied since the nineteenth century. At the end of the nineteenth and the beginning of the twentieth century, gas discharge technique was worked out which led to further development of electrical sciences, including new gas discharge devices and methods of discharge diagnostics [1]. Innovation of numerous different electrical devices contributed to discovery and development of different gas discharges, first of all atmospheric pressure discharges and then different varieties of low-pressure discharges (arc, corona, glow, rf and microwave discharges, dielectric barrier discharges etc.) [1–6]. Due to wide diversity of electrical gas discharges and abilities of easy modification of basic parameters (type of gas and cathode material, size and separation of electrodes, pressure, dimension of the vessel…), the field of their application has rapidly expanded. Nowadays, gas discharges are widely used in different areas of science and technology for surface treatments, plasma displays, gas switches, for polymer and novel materials

generation, in timing devices, nanotechnology, also for biomedical and environmental applications, etc. [3, 4, 7–12].

The rapid development of gas discharge devices and methods and increased range of their application required a detailed study of the characteristic processes and phenomena. The majority of processes that occur during the electrical discharges have a stochastic character and therefore the application of statistical methods is inevitable and very appropriate [5, 12–20]. The statistical analysis is particularly suitable for breakdown voltage and time delay measurements in experiments on electrical breakdown of gases, where electrical breakdown denotes the gas transition from a non-self-sustaining to a self-sustaining discharge.

Time delay measurements are based on the fact that transition of gases into a conducting state is not instantaneous. The electrical breakdown in gases always occurs with a certain delay in regard to the moment of voltage application to the gas tube. A time interval between the moment of application of voltage greater than the static breakdown voltage U_s (the lowest voltage which may cause gas breakdown at the given experimental conditions, providing the presence of initiating electron(s) [1]) and the electrical breakdown occurrence is the breakdown time delay t_d. It comprises statistical t_s and formative time delay t_f ($t_d = t_s + t_f$). The statistical time delay t_s is the time elapsed from voltage application to the appearance of initiating electron(s), while the discharge formation time t_f is the time needed the ionization to increase enough to cause the breakdown, *i.e.*, to cause the collapse of the applied voltage and occurrence of a self-sustained current [21].

According to definition, the statistical time delay is stochastic variable because the appearance of electron(s) that may initiate the discharge depends on amount of pre-ionization and irradiation of interelectrode space. The stochastic character of statistical time delay was experimentally proved by Zuber [22], while von Laue [23] derived the exponential distribution for its theoretical description. In the original form, Laue theory is derived for low level of electron density and in terms of steady-state (stationary) conditions of the considered physical system. The Laue diagrams obtained in such conditions are straightened and by their analysis correct description of experimental data could be made. However, the type of t_s distributions depends on pre-ionization levels, *i.e.*, on the electron yields *Y*. The distributions of statistical time delay are exponential ones only for the low pre-ionization (the rare independent events) and change to the Gauss-exponential and Gaussian ones when the electron yields Y increase [16, 20, 24].

The cumulative exponential distribution of t_s derived by Kiselev [25]:

$$F_E(t_s) = 1 - \exp\left(-\frac{t_s}{\bar{t}_s}\right) = 1 - \exp\left(-YPt_s\right) \tag{1}$$

has the mean value of the statistical time delay $\bar{t}_s$ as a distribution parameter. The $\bar{t}_s$ is the inverse of the effective electron yield $\bar{t}_s = 1/Y_{eff} = 1/YP$, where P is the breakdown probability of one electron to cause a breakdown [13, 21]. In semi-logarithmic representation (Laue plot), the exponential distribution of the statistical time delay under stable conditions is straightened, because the electron yield Y and the breakdown probability P are constant [26]. However, the Laue theory in its genuine form is used although the experimental condition have not been always stationary. Under unstable conditions (desorption of adsorbed gases and impurities, sputtering of nonhomogeneous layers or oxides) [27] or time varying voltage pulses [17, 18], Y and/or P are time dependent variables. In such cases, the Laue plots are curved to the lower or higher values of the statistical time delay and it is necessary to introduce the nonstationary distributions of t_s with time dependent parameters.

The formative time t_f, as a part of breakdown time delay t_d, has own stochastic [19, 24, 28–32] expressed by the Gaussian distribution which was confirmed in different experiments [24, 32]. In the case of high level of residual states, the discharge formation time t_f is the dominant part of time delay t_d because the statistical time delay t_s and its fluctuations $\sigma(t_s)$ are reduced to the negligible values in comparison with t_f and $\sigma(t_f)$. On the other hand, at low pre-ionization, the formative time delay, as well as its statistical fluctuation, is negligible and electrical breakdown time delay distributions are dominated by the statistical time delay [16, 24, 30]. Thus, the electrical breakdown experiments with low level of residual states, *i.e.*, with low rate of electron production Y enable the study of the statistical time delay and its distributions.

In this paper we analyzed the application of nonstationary exponential distribution of statistical time delay in the case of argon DC discharge under unstable experimental conditions. Details related to the experiment are described in section 2. In the third section the nonstationary exponential distribution with time dependent parameter, that reflects time dependent experimental conditions, is derived based on binomial distribution for rare independent electron occurrence in the gap. By introducing the nonstationary exponential distribution, an effort has been made to expand the Laue theory to conditions that are not constant in time, but still providing a low level of electron density. Also, the experimentally obtained data of the statistical time delay are presented in different graphical representations and modeled by the nonstationary exponential distribution, as well as by the stationary exponential and Weibull distribution for the sake of comparison. Finally, the short conclusion is given in the last section.

2. EXPERIMENTAL DETAILS

The measurements were carried out on a gas tube made of borosilicate glass (8245, Schott technical glass or molybdenum sealing glass) with the plane-parallel cylindrical OFHC (oxygen-free high thermal conductivity) unconditioned copper cathode. The radius of electrodes is R = 11 mm, front area $S = 3.8\ \mathrm{cm}^2$ and interelectrode distance d = 20 mm. Both electrodes, prior to their installation in the tube, were lapped and polished with polishing paste (grain size $1\ \mu\mathrm{m}$), cleaned in ultrasonic bath in ethanol and then in distilled water. The roughness of the front electrode surface was measured on MarSurf XR 1 profilometer and it was found that the mean value of root-mean-square surface roughness was $R_M = 0.020\ \mu\mathrm{m}$. The electrodes have slightly rounded edges in order to avoid edge effects and electric field inhomogeneity. The tube was evacuated down to the pressure of $10^{-5}\ \mathrm{Pa}$, baked at $600\ \mathrm{K}$ and afterwards filled with argon (Matheson Co. 99.9999 % research purity argon with a nitrogen impurity below 1 ppm) at the pressure of 200 Pa. The time delay measurements were carried out by applying a series of high-voltage rectangular ("step") voltage pulses (with rise time of $0.18\ \mu\mathrm{s}$) to the tube with the unconditioned electrode surfaces covered with sooth, oxides and adsorbed particles. One hundred breakdown time delays were measured for every working voltage U_w. The static breakdown voltage was $U_s = 250$ V, glow current $I_g = 70\ \mu\mathrm{A}$ and glow time $t_g = 1\ \mathrm{s}$, long enough to establish steady-state glow discharge conditions. The afterglow period *i.e.*, time between the voltage pulses was $\tau = 1\ \mathrm{s}$ providing low level of residual states. During the measurements the tube was protected from external light. The experimental distributions of t_s, at different working voltages U_w, are obtained by subtracting $t_f \approx t_{d\min}$ from the measured time delay values [16, 24, 33]. More details about the experimental procedure, measuring system and tube preparation can be found in Marković [34].

3. RESULTS AND DISCUSSION

The statistical time delay is random variable with the cumulative distribution function $F(t_s)$ which is determined by the probability of occurrence at least one electron in the interelectrode space for the time interval t_s [25]. In other words, the electrical breakdown of gases could happen if one or more electrons have occurred during the time t_s. The breakdown probability depends on amount of pre-ionization or irradiation of interelectrode space and in accordance with probability

theory, it is equal to the sum of probabilities of occurrence of k electrons in the interelectrode space. This discrete distribution of electron occurrence passes into a homogeneous continuous one for waiting time t_s until the first effective electron appears (electron which initiates successful avalanche) [20, 24]. In the case of stable discharge conditions (*e.g.*, electrical breakdowns by "step" pulses with negligible sputtering) when the process of electron appearance is a stationary one, the electron yield Y and the breakdown probability P are not time dependent, so the statistical time delay distribution, for the rare independent events, is the stationary exponential one (1). This distribution is linearized in Laue representation:

$$\ln\left(\frac{n}{N}\right) = -\frac{t_s}{\bar{t}_s} = -YPt_s\,, \tag{2}$$

where n/N is relative fraction of delay times greater than t_s, and from the slope of the Laue diagram the electron yield can be derived $Y = -(1/P)\ln(n/N)/t_s$ [26].

As already mentioned, P represents the breakdown probability of one electron to cause a breakdown [13, 21] and in Townsend model it is given by Wijsman relation [13]:

$$P = \begin{cases} 0 \text{ for } q < 1 \\ 1 - 1/q \text{ for } q > 1. \end{cases} \tag{3}$$

In relation (3), $q = \gamma\left[\exp(\alpha d) - 1\right]$ denotes electron multiplication factor, γ is the secondary electron yield (number of electrons emitted by incident ion) and α is the electron ionization coefficient (number of ionization events by an electron in a 1 cm path along the field) [1, 21]. The last coefficient is expressed by the semi-empirical relation [35] as a function of reduced electric field E/N (ratio of electric field and the gas density) obtained by fitting of the various experimental data.

Based on the previous discussion, it is obvious that in the case of electrical breakdowns by "step" pulses (constant working voltages) with negligible cathode sputtering, time delay distributions could be described by relation (1) with stationary distribution parameter $\bar{t}_s = 1/YP$. However, during the gas breakdown, nonstationary processes could happen such as sputtering of nonhomogeneous layers or oxides, desorption of adsorbed gasses and impurities, etc. In those cases, as well as in the case of application of time varying voltage pulses, the electron yield and/or the breakdown probability are time dependent variables and the statistics of the electrical breakdowns is a nonstationary one. Thus, when the electrical breakdown occurs under unstable conditions, it is necessary to introduce the nonstationary distribution of t_s with time dependent parameter. For its

derivation, first we need to define the cumulative electron yield $\beta(t)$ under nonstationary conditions when the electron yield $Y(t)$ and the breakdown probability $P(t)$ are time dependent variables:

$$\beta(t) = \int_0^{t_s} Y(t) P(t) \mathrm{d}t. \tag{4}$$

Next, we divide the time interval t_s to a large number m of the subintervals $\Delta t = t_s / m$, where each subinterval Δt could be consider as infinitely small. In this way, the term $\beta(t)/m$ expresses the probability of occurrence of an effective electron in the time interval Δt, while the probability of electron non-occurrence is $1-\beta(t)/m$. In addition, we suppose that parameter m represents a maximum number of occurred electrons, which is equal to the number of subintervals, in order to obtain at most an accident in each subinterval (independent accidents). As in the stationary case, the electrical breakdown of interelectrode space could happen if one or more electrons have appeared during the time interval t_s. Thus, the probability of breakdown W in the time interval t_s can be derived from binomial distribution of electron occurrence *i.e.*, the probability is equal to the sum of the probabilities of occurrence of k electrons in the interelectrode space:

$$W = \sum_{k=j}^{m} C_m^k \left(\frac{\beta(t)}{m} \right)^k \left(1 - \frac{\beta(t)}{m} \right)^{m-k}, \tag{5}$$

where k takes all integer values in the interval $[j-m]$ and C_m^k are the binomial coefficients. When m is large enough ($m \to \infty$) and at least one electron occurs in the interelectrode space (probability of electron occurrence $\beta(t)/m \equiv p$ is close to zero and $j = 1$ [16, 20, 36]) the terms under the sign of summation go into Poisson distribution:

$$W = \sum_{k=1}^{\infty} \frac{[\beta(t)]^k}{k!} \mathrm{e}^{-\beta(t)} =$$

$$= \mathrm{e}^{-\beta(t)} \left[\frac{\beta(t)}{1!} + \frac{\beta^2(t)}{2!} + \frac{\beta^3(t)}{3!} + \cdots \right]. \tag{6}$$

After the summation in relation (6), the power series in parentheses turns into $\exp[\beta(t)]-1$, and the sum (6) goes into a continuous time distribution *i.e.*, the cumulative nonstationary exponential distribution of the statistical time delay, for the rare independent events is obtained:

$$F_E(t_s) = 1 - \mathrm{e}^{-\beta(t)} = 1 - \exp\left[-\int_0^{t_s} Y(t)P(t)\mathrm{d}t \right]. \quad (7)$$

On the other hand, when $m \to \infty$ but either p or $(1-p)$ is not close to zero, sum of discrete binomial distributions (5) can be approximated by the Gaussian or Gauss-exponential distribution [16, 20, 36].

Taking into account the connection between relative fraction n/N of delay times greater than actual time t_s and cumulative distribution $F_E(t_s)$, Laue representation of nonstationary exponential distribution gets the form:

$$\ln\left(\frac{n}{N}\right) = \ln\left[1 - F_E(t_s)\right] = -\int_0^{t_s} Y(t)P(t)\mathrm{d}t\,. \quad (8)$$

Also, based on relation (7), the nonstationary exponential density distribution function $f_E(t_s)$ is expressed as:

$$f_E(t_s) = \frac{\mathrm{d}F_E(t_s)}{\mathrm{d}t} = Y(t)P(t)\exp\left[-\int_0^{t_s} Y(t)P(t)\mathrm{d}t \right]. \quad (9)$$

The nonstationary exponential distributions of the statistical time delay (7–9) are applied for theoretical description of nonstationarity during the measurements and the good agreement with the experimental data is found.

The experimental data in Laue representation are shown in Figs. 1 and 2. In these figures, the measurements obtained at different working voltages are presented and modeled by nonstationary distribution (8). Moreover, the Laue diagrams are modeled by stationary exponential distribution and two-parameter Weibull distribution for the sake of comparison. At the lower working voltage $U_{w1} = 260\ \mathrm{V}$ the Laue diagram (down triangles in Fig. 1) is curved to the higher values of the statistical time delay (concave on the right), while at the higher values of the voltage $U_{w3} = 500\ \mathrm{V}$ (up triangles in Fig. 2), the curving of the Laue diagrams to the lower statistical times is obtained (convex on the right). At some intermediate voltage ($U_{w2} = 300\ \mathrm{V}$) the Laue diagram is straightened (circles in Figs. 1, 2) and this distribution is fitted by the stationary exponential one (2) with the constant distribution parameter (dashed line in Figs. 1, 2). From the slope of the linear fit of the experimental data, by using aforementioned relation $Y = -(1/P)\ln(n/N)/t_s$ the electron yield $\overline{Y_2} = 128\ \mathrm{s}^{-1}$ is obtained, where $P_2 = 0.78$ is calculated by the Wijsman's formula (3).

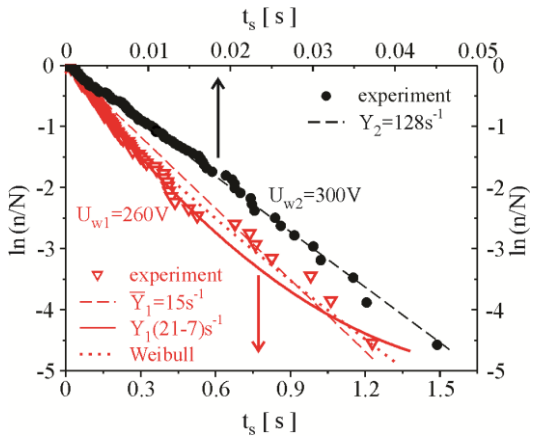

Fig. 1 – (Color online) The Laue diagrams (symbols) for $U_{w1} = 260$ V (lower scale) and for $U_{w2} = 300$ V (upper scale) and the fits based on nonstationary exponential distribution (solid line), stationary exponential distribution (dashed lines) and Weibull distribution (dotted line).

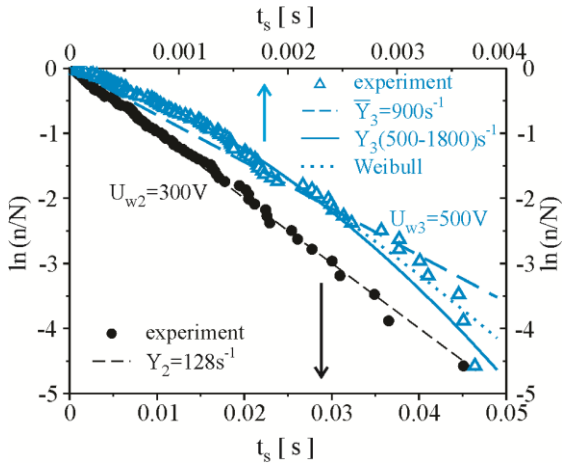

Fig. 2 – (Color online) The Laue diagrams (symbols) for $U_{w2} = 300$ V (lower scale) and for $U_{w3} = :500$ V (upper scale) and the fits based on nonstationary exponential distribution (solid line), stationary exponential distribution (dashed lines) and Weibull distribution (dotted line).

The linear fit is also applied to the curved Laue plots in Figs. 1 and 2, corresponding to the lower and higher values of working voltages. However, in that case from the slope of the linear fits of the curved diagrams, only the mean values of the electron yield $\overline{Y}$ can be calculated: $\overline{Y_1} = 15\ \mathrm{s}^{-1}$ for $U_{w1} = 260$ V and $P_1 = 0.26$ (dashed line in Fig. 1) and $\overline{Y_3} = 900\ \mathrm{s}^{-1}$ for $U_{w3} = 500$ V and $P_3 \approx 1$

(dashed line in Fig. 2). The obtained mean electron yields correspond to the application of the stationary exponential distribution (2) with constant distribution parameter $\bar{t}_s = 1/\overline{YP}$, giving the straight lines, and therefore it is inappropriate for description of the experimental data.

The curving of the Laue diagrams to the lower or higher values of the statistical time delay indicates that Y and/or P are function of time. The time dependence of the probability P is expressed through the time dependence of the secondary electron yields γ or the time dependence of the electron ionization coefficient α. Instability of γ with time can be expressed as $\gamma = \gamma_s(1 \pm ct)$, where γ_s is the secondary electron yields which correspond to the static breakdown voltage U_s [24, 34] and c is the rate constant. In the conditions of our experiment, the series of approximately one hundred breakdowns is not sufficient to produce significant changes in static breakdown voltage (variation of U_s is of the order of volts in a series), so we can assume that $c \approx 0$. Consequently, there is no significant variation in the secondary electron yields that reflects the changes in the static breakdown voltage and the variation of γ can be neglected, *i.e.* $\gamma \approx \gamma_s$. Moreover, under experimental conditions (electrical breakdowns by "step" pulses), coefficient α is a constant, in contrast to the experiments with time varying voltage pulses [17–19]. Therefore the time dependence of breakdown probability is negligible *i.e.*, $P \approx \text{const.}$ and for theoretical description of mildly curved Laue diagrams is sufficient to take into account only variation of electron yield Y.

Since the experimentally obtained Laue diagrams of statistical time delay are slightly curved, the slowly varying electron yield is proposed. The variability of Y with time can be represented by:

$$Y_i = Y_{0i}(1 \pm \lambda_i t) \tag{10}$$

which describes the increasing or decreasing electron yield due to unstable conditions during the discharge such as roughening and smoothing effect on the cathode due to sputtering, or adsorption of nonhomogeneous layers or oxides, desorption of adsorbed gasses and impurities, etc. The parameters λ_i in relation (10) are the growth/decay constants and their values could be obtained as fitting parameters.

The fitting of the experimental data in Fig. 1, for the voltage U_1 = 260 V is carried out by using the linearly decreasing function of the electron yield: $Y_1 = Y_{01}(1 - \lambda_1 t)$ with the fitting parameters $Y_{01} = 21\ \text{s}^{-1}$ and $\lambda_1 \approx 0.55\ \text{s}^{-1}$ (Fig. 1, solid line). However, the experimental data in Fig. 2 for the voltage U_3 = 500 V require the use of linearly increasing yield: $Y_3 = Y_{03}(1 + \lambda_3 t)$ with the fitting parameters $Y_{03} = 500\ \text{s}^{-1}$ and $\lambda_3 \approx 700\ \text{s}^{-1}$ (solid line in Fig. 2). Slight deviation of the experimental data from the relation (8) (solid lines in Figs. 1 and 2) might be

due to insufficient number of measurements in a series, but with increasing number of measurements effect of down and up curving of Laue diagrams would be less pronounced. Also, the adsorbed impurities and oxides may increase the statistical spread.

Based on data modeling process, it was determined that the unconditioned copper cathode surface shows reduced surface emissivity at lower working voltages (decreasing electron yield) but, when electrical breakdowns happen at higher voltages, the emissivity of unconditioned cathode grows up (increasing electron yield). Rising cathode emissivity indicates the "roughing" effect of high voltages because of cathode sputtering during the glow discharge. Impacting species with sufficient energy induce collision cascades that lead to the particle ejection from the cathode surface [3], whereby copper and its oxides show high sputtering yield (number of ejected particles per incident particle), *i.e.*, increased sputtering rate at higher voltages [37–41]. That way, the different surface defects, micro-protrusions, micro-craters are produced behaving as the electron traps or retaining the surface charges in the more extent and consequently the cathode emissivity grows up. Also, increased roughness, as well as the presence of a layer of different impurities, oxides or other irregularities on the cathode surface (unconditioned surface) could locally enhance the applied electric field and thus increase cathode emissivity [42, 43]. Possible explanation of decreasing electron yield at low operating voltages is "smoothing" of copper cathode surface caused by the particle bombardment, as well as redeposition, back diffusion (back-sputtering) of sputtered material or agglomeration of adatoms [38, 44–47]. Moreover, during the discharge, the ions that reach cathode surface have a wide energy range because they originate from different parts of the cathode fall. Consequently, they have a wide angular distribution. At low working voltages, the higher incident angle of ions is predominant and smoothing effect, too [48].

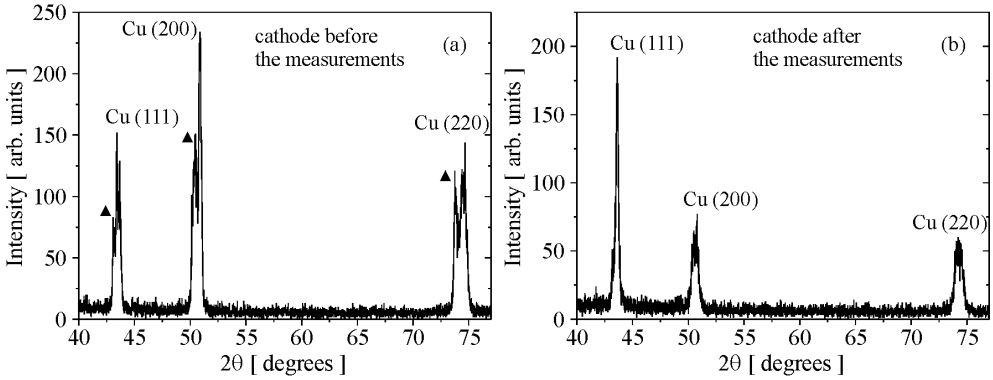

Fig. 3 – X-ray diffraction pattern of the copper cathode surface: a) cathode before the measurements with the peaks of pure copper [Cu(111), Cu(200) and Cu(220)] and copper oxides (denoted by ▲); b) cathode after the large number of measurements with the peaks of pure copper only.

Accordingly, by changing the electrical breakdown conditions, surface modification for different purposes can be done, such as surface modification for sample preparation due to microstructure investigation and layer analysis, for spectrochemical analysis, surface preparation because of improvement of the SEM image quality, for thin films production, for surface reflectivity changing, surface cleaning [38, 47, 49–51], etc. Removing of copper oxides, by the cathode sputtering during the glow discharge in our experiment, is confirmed by X-ray diffraction (XRD) analyses of the cathode surface. The XRD technique is particularly suitable for identification and characterization of surface compounds. The XRD plot of unconditioned cathode shows, in addition to peaks corresponding to the pure copper, the peaks (Fig. 3a) that can be related to the presence of the copper oxides [52, 53]. However, such analysis of the cathode after the conditioning shows the peaks of the pure copper only (Fig. 3b).

The previous analysis shows that the conditioning of the cathode surface (removing of oxides, adsorbed species and/or different kind of impurities) is very important part of glow discharge experiment preparation. The use of unconditioned cathode leads to different surface conditions in each subsequent breakdown. Such nonstationary conditions on the unconditioned cathode surface are manifested by curved Laue plots in terms of low preionization levels when straightened diagrams are expected. To achieve stable experimental conditions, the cathode surface conditioning is necessary by running the glow discharge for few hours and several thousands of breakdowns.

Since, Weibull distribution is often used for description of stochastic processes in solids, liquids and gases [54–57], the two-parameter Weibull distribution [58] is applied for modeling of the experimental data, as a comparison. From the Weibull probability density function:

$$f(t_s) = \frac{\xi}{\eta}\left(\frac{t_s}{\eta}\right)^{\xi-1} \exp\left[-\left(\frac{t_s}{\eta}\right)^{\xi}\right], \tag{11}$$

with ξ as the shape and η as the scale distribution parameter, the Laue representation is given and applied to the Laue diagrams in Figs. 1 and 2. The best fit of the data for $U_1 = 260$ V is obtained with parameters $\xi = 0.835$ and $\eta = 0.201$ s (dotted line in Fig. 1), while for the voltage $U_3 = 500$ V the best agreement of the Weibull distribution with the experiment is accomplished with parameters $\xi = 1.318$ and $\eta = 1.33 \cdot 10^{-3}$s (dotted line in Fig. 2). However, these parameters do not have physical meaning and in spite of good agreement with the experimental data, the use of Weibull distribution for interpretation of physical processes is unsuitable.

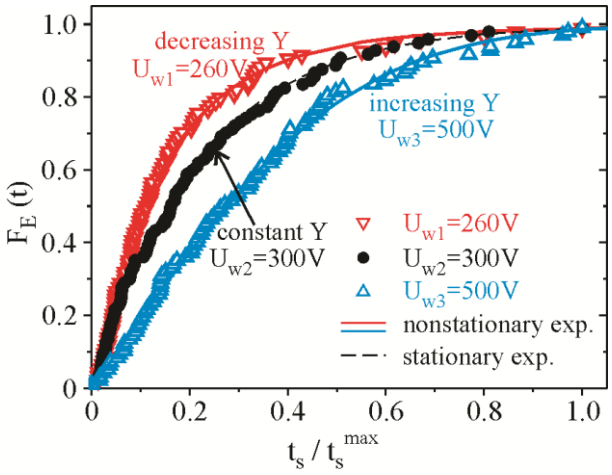

Fig. 4 – (Color online) The experimental cumulative distributions of the statistical time delay for different working voltages (symbols), the fits based on nonstationary exponential distribution (7) (solid lines) and the stationary distribution (1) (dashed line).

The experimental cumulative distributions $F_E(t_s)$ of the statistical time delay are presented in Fig. 4 and fitted by the theoretical distribution (7) with the same parameters as in Figs. 1 and 2. Also, for the modeling of the data at intermediate working voltage, the stationary distribution (1) is used. As with the Laue diagrams a good agreement between nonstationary exponential distribution and experimental data is observed in this graphical representation.

The experimental density distributions $f_E(t_s)$ of the statistical time delay t_s are shown in Fig. 5. The represented experimental data are obtained for different working voltages, but for the same relaxation time $\tau = 1$ s that is characterized by low level of residual states and therefore exponential distributions are expected. The histogram in Fig. 5b obtained at $U_2 = 300$ V has expected exponential shape (straightened Laue diagram in Figs. 1 and 2) and it is modeled by stationary exponential distribution presented by dashed line.

However, the t_s density distribution at lower $U_1 = 260$ V (Fig. 5a) and higher working voltages $U_3 = 500$ V (Fig. 5c) deviate from exponential form. The histogram in Fig. 5a shows prominent right "tail" which correspond to the curving of the Laue diagram to the higher values of the statistical time delay (Fig. 1) due to reduced surface emissivity (decreasing electron yield at lower U_w). On the other hand, the histogram obtained at higher working voltages has more pronounced central part, which corresponds to the curving of the Laue diagram to the lower values of t_s (Fig. 2) due to increasing cathode emissivity (increasing electron yield).

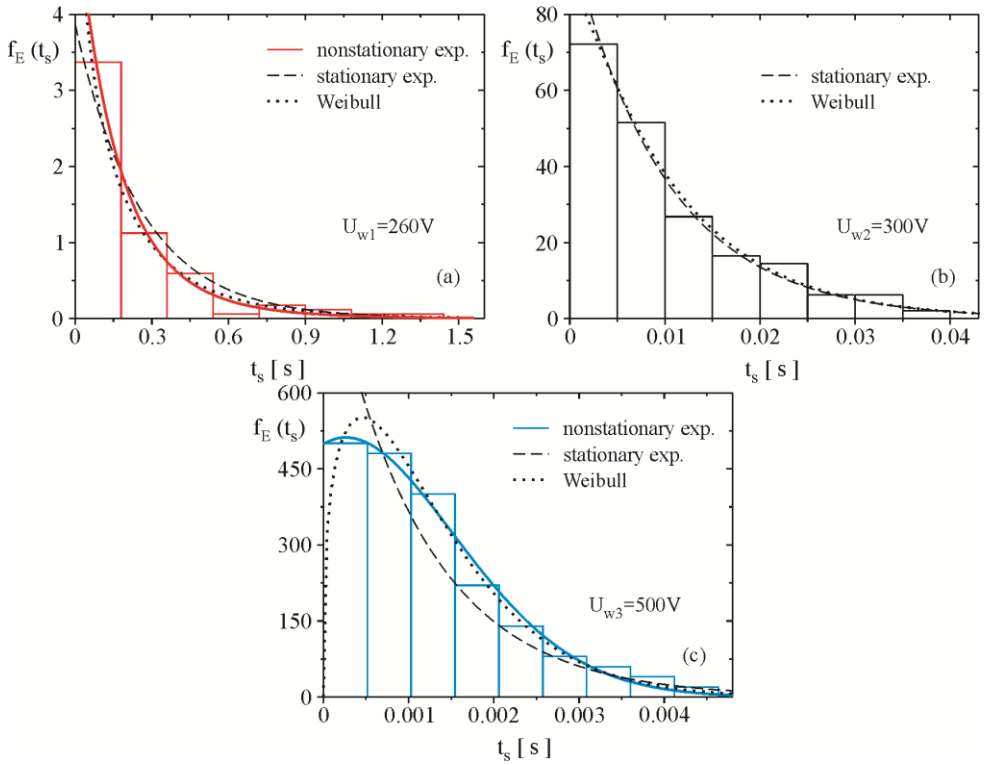

Fig. 5 – (Color online) The experimental density distribution (histograms) at different working voltages, fitted by nonstationary exponential distribution (solid lines), stationary exponential (dashed lines) and Weibull distribution (dotted lines).

Modeling of last two aforementioned histograms by stationary exponential function is inappropriate (dashed lines in Fig. 5a and 5b) and obtained parameters are not suitable for theoretical analysis, giving only the mean values of the electron yields. However, the deviation from the exponential shape is well described by nonstationary exponential distribution (9) with the same parameters as in the previous graphical representation of the experimental data (solid lines in Fig. 5a and 5c). The distributions also show good agreement with Weibull distribution function (dotted lines in the figure), but it should be emphasized again that its parameters have no physical meaning.

4. CONCLUSIONS

The experimental distributions of statistical time delay t_s in argon DC glow discharge with unconditioned copper cathode surface and low pre-ionization level

are presented. Obtained distributions deviate from the expected exponential ones due to unstable experimental conditions. The nonstationary exponential distribution with time dependent parameters, that reflects nonstationary experimental conditions, is derived based on binomial distribution for rare independent electron occurrence in order to fit the measured distributions. The curving of the Laue diagrams to the higher values of the statistical time delay (concave on the right) at low working voltages is described by decreasing electron yield Y in the interelectrode space (smoothing effect). However, the increasing electron yield Y is used for modeling of curved Laue diagrams to the lower values of the statistical time delay (convex on the right) at higher voltages (roughening effect). The fitting of the experimental statistical time delay distributions by stationary exponential ones is inadequate and obtained distribution parameters are incomplete, giving only the mean value of the electron yield, while in the case of Weibull distributions the parameters do not have physical meaning. Therefore, for rare independent events at slowly varying experimental conditions, we suggest to apply physically based nonstationary exponential distribution with parameters that quantify properly physical processes.

Acknowledgements. The authors are grateful to Ministry of Education, Science and Technological Development of the Republic of Serbia for partial support (project 171025), as well as to P. Janković, from the Faculty of Mechanical Engineering, for the profilometer measurements and R. Vasiljković from the Faculty of Physic (Belgrade) for XRD measurements.

REFERENCES

1. Yu.P. Raizer, *Gas discharge physics*, Springer-Verlag, Berlin, 1991.
2. M.J. Druyvesteyn, F.M. Penning, Rev. Mod. Phys. **12**, 87-174 (1940).
3. B.N. Chapman, *Glow discharge processes: sputtering and plasma etching*, John Wiley and Sons, New York, 1980.
4. A. Bogaerts, E. Neyts, R. Gijbels, J. van der Mullen, Spectrochim. Acta. Part B **57**, 609-658 (2002).
5. G.G. Raju, *Gaseous electronics: theory and practice*, CRC Press, Taylor & Francis Group, Boca Raton, 2006.
6. W.G. Huo, S.J. Jian, and Z.F. Ding, Phys. Plasmas **21**, 053505 (2014).
7. G.G. Lister, J.E. Lawler, W.P. Lapatovich, V.A. Godyak, Rev. Mod. Phys. **76**, 541-598 (2004).
8. M.A. Lieberman, A.J. Lichtenberg, *Principles of plasma discharges and materials processing*, John Willey & Sons, New Jarsey, 2005.
9. T. Makabe, Z.Lj. Petrović, *Plasma Electronics: Applications in Microelectronic Device Fabrication*, CRC Press, Taylor & Francis Group, New York, 2006.
10. A. Fridman, *Plasma chemistry*, Cambridge University Press, Cambridge, New York, 2008.
11. M. Meyyappan, J. Phys. D: Appl. Phys. **44**, 174002 (2011).
12. M. Brasoveanu, M.R. Nemtanu, C Surdu-Bob, G. Karaca, I. Erper, Romanian Reports in Physics, **67**, 617-624 (2015)
13. R.A. Wijsman, Phys. Rev. **75**, 833-838 (1949).
14. F.L. Jones, Proc. Phys. Soc. B **62**, 366-376 (1949).
15. J. Moreno, M. Zambra, M. Favre, IEEE Trans. Plasma Sci. **30**, 417-422 (2002).

16. V.Lj. Marković, S.R. Gocić, S.N. Stamenković, J. Phys. D: Appl. Phys. **39**, 3317-3322 (2006).
17. S.N. Stamenković, S.R. Gocić, V.Lj. Marković, A.P. Jovanović, J. Appl. Phys. **110**, 103304 (2011).
18. A. Sobota, J.H.M. Kanters, E.M. van Veldhuizen, F. Manders, M. Haverlag, J. Appl. Phys. **44**, 135203 (2011).
19. J. Foster, H. Krompholz, A. Neuber, Phys. Plasmas **18**, 013502 (2011).
20. V.Lj. Marković, A.P. Jovanović, S.N. Stamenković, B.Č. Popović, EPL **100**, 45002 (2012).
21. C.G. Morgan, Irradiation and time lags, in: J.M. Meek, J.D. Craggs (Eds.), *Electrical Breakdown of Gases*, John Wiley & Sons, Chichester, 1978, pp. 655-688.
22. K. Zuber, *Über die verzögerungszeit bei der funkenentladung*, Ann. Phys. **381**, 231-260 (1925).
23. M. von Laue, Bemerkung zu K. Zubers, *Messung der Verzögerungszeiten bei der Funkenentladung*, Ann. Phys. **381**, 261-265 (1925).
24. V.Lj. Marković, S.R. Gocić, S.N. Stamenković, J. Phys. D: Appl. Phys. **42**, 015207 (2009).
25. J.V. Kiselev, *Proc. 7th Int. Conf. Phenomena in Ionized Gases* (in Russian), Belgrade (Yugoslavia), 1965, p. 838.
26. V.Lj. Marković, S.R. Gocić, M.K. Radović, Eur. Phys. J Appl. Phys. **6**, 303-307 (1999).
27. G.M. McCracken, Vacuum **24**, 463-467 (1974).
28. G.A. Kachickas, L.H. Fisher, Phys. Rev. **91**, 775-779 (1953).
29. H. Tagashira, S. Sakamoto, Brit. J. Appl. Phys. (J. Phys. D) **2**, 1193-1201 (1969).
30. V.Lj. Marković, S.N. Stamenković, S.R. Gocić, S.M. Đurić, Eur. Phys. J Appl. Phys. **38**, 73-78 (2007).
31. K. Yoshino, T. Nagatomi, Y. Morita, T. Oue, N. Kosugi, M. Nishitani, M. Kitagawa, Y. Takai, Jpn. J. App. Phys. **50**, 026201 (2011).
32. V.Lj. Marković, B.Č. Popović, A.P. Jovanović, S.N. Stamenković, M.N. Stankov, EPL **109**, 15002-p1-p6 (2015).
33. V.Lj. Marković, Z.Lj. Petrović, M.M. Pejović, Plasma Sources Sci. Technol. **6**, 240-246 (1997).
34. V.Lj. Marković, S.R. Gocić, S.N. Stamenković, Z.Lj. Petrović, Phys. Plasmas **12**, 073502 (2005).
35. A.V. Phelps, Z.Lj. Petrović, Plasma Sources Sci. Technol. **8**, R21-R44 (1999).
36. M.R. Spiegel, *Schaum's outline of theory and problems of Probability and Statistics*, McGraw-Hill Book Company, New York, 1988.
37. H.H. Andersen, Radiat. Eff. **7**, 179-186 (1971).
38. P.W.J.M. Boumans, Anal. Chem. **44**, 1219-1228 (1972).
39. J.P. Biersack, Nucl. Instrum. Methods Phys. Res. **B27**, 21-36 (1987).
40. N. Matsunami, O. Fukuoka, M. Tazawa, H. Kakiuchida, M. Sataka, Surf. Coat. Technol. **203**, 2642-2645 (2009).
41. N. Matsunami, Y. Sakuma, M. Sataka, S. Okayasu, H. Kakiuchida, Nucl. Instrum. Methods Phys. Res. B **314**, 55-58 (2013).
42. F. Llewellyn Jones, D.J. Nicholas, Brit. J. Appl. Phys. **13**, 514-520 (1962).
43. V.I. Kristya, Y.N. Tun, J. Surf. Invest. **9**, 280-285 (2015).
44. D.E. Harrison, P.W. Kelly, B. Garrison, N. Winograd, Surf. Sci. **76**, 311-322 (1978).
45. V. Naundorf, M.P. Macht, Nucl. Instrum. Methods **168**, 405-409 (1980).
46. W.W. Harrison, C.M. Barshick, J.A. Klinger, P.H. Ratliff, Y. Mei, Anal. Chem. **62**, 943A-949A (1990).
47. V. Brackmann, V. Hoffmann, A. Kauffmann, A. Helth, J. Thomas, H. Wendrock, J. Freudenberger, T. Gemming, J. Eckert, Mater. Charact. **91**, 76-88 (2014).
48. T. Hino, T. Nakai, M. Nishikawa, Y. Hirohata, and Y. Yamauchi, J. Vac. Sci. Technol. B **24**, 1918-1921 (2006).
49. K. Shimizu, T. Mitani, *New horizons of applied scanning electron microscopy*, Springer Science & Business Media, Berlin, 2010.
50. D. Rönnow, J. Isidorsson, G. A. Niklasson, Phys. Rev. E **54**, 4021-4026 (1996).
51. E.A.O. Saettonne, J.A.S. da Matta, W. Alva, J.F.O. Chubaci, M.C.A. Fantini, R.M.O. Galvao, P. Kiyohara, M.H. Tabacniks, J. Phys. D: Appl. Phys. **36**, 842-848 (2003).

52. M. Yin, C.K. Wu, Y. Lou, C. Burda, J.T. Koberstein, Y. Zhu, S. O'Brien, J. Am. Chem. Soc. **127**, 9506-9511 (2005).
53. Q. Bao Zhang, D. Xu, T.F. Hung, K. Zhang, Nanotechnology **24**, 065602 (2013).
54. W. Weibull, J. Appl. Mech. **18**, 293-297 (1951).
55. R.H. Doremus, J. Appl. Phys. **54**, 193-198 (1983).
56. R.A. Schlitz, K. Yoon, L.A. Fredin, Y. Ha, M.A. Ratner, T.J. Marks, L.J. Lauhon, J. Phys. Chem. Lett. **1**, 3292-3297 (2010).
57. C. Lu, R. Danzer, F. D. Fischer, Phys. Rev. E **65**, 067102 (2002).
58. N.L. Johnson, S. Kotz, N. Balakrishnan, *Continuous Univariate Distributions*, Vol. 1, John Wiley and Sons, New York, 1994.